

Preprint

Accepted paper at IEEE HPSR 2026

© 2026 IEEE. Personal use of this material is permitted. Permission from IEEE must be obtained for all other uses, in any current or future media, including reprinting/republishing this material for advertising or promotional purposes, creating new collective works, for resale or redistribution to servers or lists, or reuse of any copyrighted component of this work in other works.

Until published, please cite as:

Sarpkaya, F. B., Francini, A., Erman, B., Panwar, S., Evaluation of TCP Congestion Control for Public High-Performance Wide-Area Networks, Proc. 27th International Conference on High Performance Switching and Routing, IEEE HPSR 2026, Montreal, Canada, June 2026, in print.

Evaluation of TCP Congestion Control for Public High-Performance Wide-Area Networks

Fatih Berkay Sarpkaya¹, Andrea Francini², Bilgehan Erman², Shivendra Panwar¹

¹*NYU Tandon School of Engineering, Brooklyn, NY, USA*

²*Nokia Bell Labs, Murray Hill, NJ, USA*

fbs6417@nyu.edu, andrea.francini@nokia-bell-labs.com, bilgehan.erman@nokia-bell-labs.com, panwar@nyu.edu

Abstract—Practitioners of a growing number of scientific and artificial-intelligence (AI) applications use High-Performance Wide-Area Networks (HP-WANs) for moving massive data sets between remote facilities. Accurate prediction of the flow completion time (FCT) is essential in these data-transfer workflows because compute and storage resources are tightly scheduled and expensive. We assess the viability of three TCP congestion control algorithms (CUBIC, BBRv1, and BBRv3) for massive data transfers over *public* HP-WANs, where limited control of critical data-path parameters precludes the use of Remote Direct Memory Access (RDMA) over Converged Ethernet (RoCEv2), which is known to outperform TCP in *private* HP-WANs. Extensive experiments on the FABRIC testbed indicate that the configuration control limitations can also hinder TCP, especially through microburst-induced packet losses. Under these challenging conditions, we show that the highest FCT predictability is achieved by combination of BBRv1 with the application of traffic shaping before the HP-WAN entry points.

I. INTRODUCTION

Large-scale scientific applications, in fields like weather forecasting, molecular biology, and astrophysics, generate massive data sets that often cannot be processed locally. The processing capacity for these data may be located at geographically distant high-performance computing (HPC) facilities, requiring their reliable transfer across high-capacity, long-distance networks. HPC reservations are expensive and typically scheduled in advance: high accuracy in the estimation of the data transfer time, also called the *flow completion time* (FCT), improves their cost effectiveness [1]. FCT predictability is also relevant to AI applications, for example in GPU-as-a-service (GPUaaS) arrangements where users transfer massive amounts of data in and out of large-scale compute facilities before and after execution of their workloads.

We focus on FCT predictability in scenarios where the owner of the data transfer (the *user*) does not control the network infrastructure that realizes it. The prevalence of such scenarios, where network-compute capacity is offered as a service to third-party users, is growing with the set of applications that require massive transfers between remote locations, as an extension of the public-cloud business model.

Achieving predictable FCTs is a daunting challenge when sharing a public high-performance wide-area network (HP-WAN) with massive data transfers from unrelated users.

Fatih Berkay Sarpkaya was with Nokia Bell Labs, Network Systems and Security Research, Murray Hill, NJ (USA) when this work was performed.

First, given the size of the data file, an accurate estimate of the FCT requires the capacity of the network path to be known and stable in time, as offered by a virtual circuit (VC) with fixed guaranteed bandwidth. Such an isolated network traversal service can be realized through various combinations of traffic management functions like packet scheduling, traffic policing, traffic shaping, flow control, and congestion control, and traffic engineering functions like explicit routing and admission control. Given the variety of the combinations and the lack of user control over their configuration, the ideal behavior of the data transfer endpoints is one that performs robustly under a general assumption of bandwidth isolation.

Second, a reliable end-to-end transport, as offered by the Transport Control Protocol (TCP), must be used to systematically avoid data losses. Harnessing TCP requires the selection of a congestion control (CC) algorithm that provides consistent throughput performance under the large bandwidth-delay-product (BDP) conditions of the HP-WAN VC. Alternatives to TCP exist but are not better suited to the public HP-WAN use case that we are considering. For example, the superior performance of Remote Direct Memory Access (RDMA) over Converged Ethernet (RoCEv2) [2] has been clearly proven in private HP-WAN setups [3], but cannot be reproduced in public HP-WANs, where the user cannot fine-tune the network parameters for the mandatory lossless operation of RoCEv2 [4]. QUIC enables faster connection setup and easier customization of the CC algorithm than TCP, but in the massive-transfer use case the setup time is practically negligible and a custom CC algorithm would be really needed only after all available TCP options proved inadequate.

Under generic network-path assumptions, CC algorithms are typically assessed for fairness and adaptability to varied and variable data-path conditions, including those of large-BDP network paths [5]. Conversely, the bandwidth-isolated VCs of the public HP-WAN allow us to ignore the fairness and adaptability properties and focus entirely on the predictability of the throughput performance. We study the HP-WAN viability of TCP CUBIC [6], BBRv1 [7], and BBRv3 [8] on a multi-site topology provisioned over the FABRIC research testbed [9], leveraging inter-site bandwidth-isolation capabilities that have become available with a recent upgrade of the testbed [10].

Fig. 1 shows the logical representation of the data path for massive data transfers between the endpoints. The source and destination endpoints include traffic management devices

that forward packets to and from the respective VC endpoints. In FABRIC, these devices are instantiated in software within *virtual machines* (VMs), with implementation options that include Linux traffic control tools and Data-Plane Development Kit (DPDK) [11] applications.

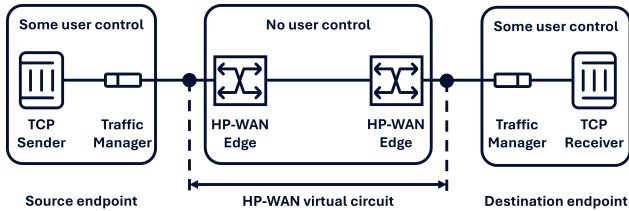


Fig. 1: Logical representation of the massive-transfer data path.

We summarize the outcomes of our experiments as follows:

- **FABRIC guarantees bandwidth isolation at scale.** On 100 Gb/s inter-site links, FABRIC enforces bandwidth reservations up to 80 Gb/s. The individual bandwidth guarantees are accurately enforced even when multiple VCs share portions of their network paths.
- **Non-congestive packet losses are common and affect the CC performance.** Despite our comprehensive optimization of user-accessible data-path and host parameters, we observe packet losses that are not correlated with delay and can degrade FCT predictability.
- **Robustness to losses is the primary criterion for CC selection.** Under non-congestive packet losses, BBRv1 provides the most stable and predictable completion times, whereas CUBIC and BBRv3 are negatively affected by those losses (CUBIC more than BBRv3).
- **DPDK outperforms kernel-based forwarding.** Relative to Linux kernel forwarding, DPDK substantially improves FCT statistics by limiting delay jitter and bursty losses.
- **Traffic shaping within the source endpoint boosts FCT predictability.** Placing traffic shapers upstream of the HP-WAN VC consistently yields high FCT efficiency and negligible overhead from packet retransmissions, outperforming all other endpoint configurations.
- **With BBRv1, data-transfer striping is not necessary for VC bandwidth up to at least 20 Gb/s.** Striping the data transfer over multiple TCP connections lowers the compute load on the TCP endpoints. It enables higher throughput but requires efficient sender-side distribution and receiver-side reordering of the packets [12]. With BBRv1, a single TCP connection fully utilizes a 20 Gb/s VC without the overhead of a striping application.

The rest of this paper is organized as follows. Section II covers prior work on our target use case, Section III describes our FABRIC setup, Section IV presents the results of our experiments, and Section V summarizes our findings.

II. BACKGROUND

HP-WANs interconnecting facilities that generate and process massive amounts of data have existed for decades, together with best practices for fine-tuning the Data-Transfer

Nodes (DTNs) that Science De-Militarized Zones (DMZs) deploy at the HP-WAN edges to optimize data movement [13]. Prominent HP-WAN examples, developed by the owners of the data generation and processing facilities that they originally interconnected, include ESnet, GÉANT, Janet, Effingo, Internet2, CANARIE, and APAN [14]. Over time, these infrastructures have been opened to a much broader set of research organizations, generating a new use case where the owner of the data transfer no longer controls the configuration of the entire end-to-end data path.

While transport optimizations for massive data transfers across public networks have already been studied [12], only minimal work exists that focuses on the particular case where bandwidth isolation is guaranteed for a large-BDP network path. The authors of [5] study the coexistence at the network bottleneck of TCP flows of different CC types under a broad range of BDP conditions and queue management policies. In our HP-WAN scenario with per-VC bandwidth isolation, fairness between CC types is out of scope because the owner of the data transfer controls the configuration of all TCP flows in the isolated VC and does not need to mix different CC types.

Our assumption of a bandwidth-isolated VC between the DTNs of the massive transfer also holds in [3], where the viability of TCP CUBIC and RoCE as HP-WAN transport options is assessed at 10 and 40 Gb/s. RDMA outperforms TCP under data-path conditions that cannot be replicated in a public HP-WAN setting. In all experiments involving TCP, the throughput of the data transfer is constrained by the capacity of the sender’s network interface card (NIC). In practical scenarios, public HP-WAN VCs must be realized with soft isolation within shared resources, with lower guaranteed bandwidth than the NIC capacities of the endpoint DTNs.

With CC algorithms that use the congestion window size (CWND) to regulate the sender data rate, it is well understood that striping the data transfer over parallel TCP connections can maximize the utilization of the bottleneck bandwidth better than a single connection [15]. We share with [16] the choice of traffic generator and load balancing tool (*iperf3*) for exploration of the benefits of TCP striping. The tool implements an ideal load balancer that equalizes the lifetime of the parallel connections independently of their actual throughput. TCP striping gains relevance in our HP-WAN scenario because complete bandwidth isolation implies the absence of competing traffic at the network bottleneck and thus eliminates all concerns about the unfairness of the striping technique [12].

III. EXPERIMENT DESIGN

We run experiments on a FABRIC testbed *slice* [9] to assess the performance of CC algorithms under typical public HP-WAN conditions, where the user has only partial control over the configuration of the end-to-end data path.

A. Fabric Slice Design

FABRIC enables the provisioning of *Layer-2 Point-to-Point* (L2PTP) VCs with guaranteed bandwidth between Mellanox ConnectX-6 SmartNICs at remote sites [10]. The instantiation

of a slice succeeds only if the bandwidth requested for its L2PTP VCs is available on all links of their explicitly assigned paths. The bandwidth is then subtracted from the pool left available for future reservations. At runtime, a *hard policer* at the entry point of the VC (the edge-router ingress port that faces the SmartNIC) tightly caps the guaranteed bandwidth of the VC: the policer immediately drops every incoming packet that violates the leaky-bucket profile of the VC without applying color marking [17]. The burst size of the profile is not accessible for configuration. Relying on the hard enforcement of bandwidth caps at the ingress edge, FABRIC assigns all L2PTP packets to a single *expedited forwarding* (EF) queue [18]. The EF queue holds the highest service priority and is shaped at about 80% of the link capacity independently of the cumulative reservations of the L2PTP VCs it carries.

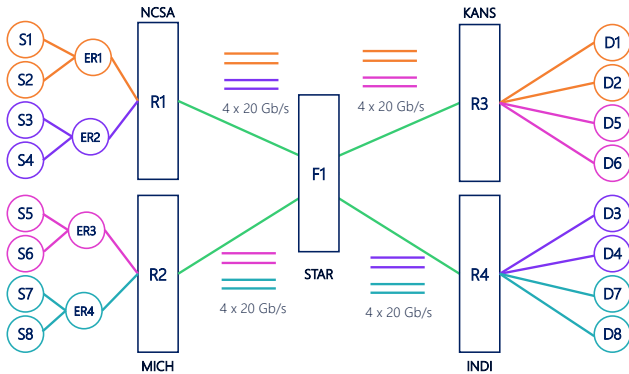


Fig. 2: Slice topology; L2PTP VCs terminate on router VMs R1–R4.

Figure 2 shows the topology of our slice. Eight sender DTNs at two source sites (NCSA in Illinois and MICHigan) transmit large data files to respective receiver DTNs (in KANSas and INDIana) over high-capacity VCs with non-negligible propagation delay. A central site (STARlight in Illinois) interconnects the source and destination sites. Sender-receiver VCs form pairs with the same base round-trip time (RTT): 14 ms for $S1-2 \longleftrightarrow D1-2$, 7 ms for $S3-4 \longleftrightarrow D3-4$, 16 ms for $S5-6 \longleftrightarrow D5-6$, and 10 ms for $S7-8 \longleftrightarrow D7-8$. The topology and VC configuration are intended to produce inter-VC interference at every stage of the data path.

In experiments with the full topology of Fig. 2, the maximum bandwidth reservation of every VC is 20 Gb/s, to comply with the 80 Gb/s reservation limit on the 100 Gb/s links of FABRIC ($R1-4 \longleftrightarrow F1$). In system-limit experiments (Section IV-A), we use a single 80 Gb/s VC between two sites.

Due to the limited availability of SmartNICs at individual FABRIC sites (typically eight or less), it is hard to find four SmartNICs (one per VC) simultaneously available for reservation at each of the four sites that host VC terminations. We gain ease of slice creation at the cost of increased exposure to cross-traffic interference by associating all VC terminations at each site with a single SmartNIC. Accordingly, in each source site (NCSA and MICH), we instantiate the DTNs in respective VMs (S1–4 and S5–8), group them in two pairs per site, and assign each pair to a distinct host. Each source DTN

host includes an edge-router VM (ER1–4) for the optional insertion of traffic shaping between the DTNs and the host of the local SmartNIC, where a router VM (R1–2) forwards the traffic to and from the VC endpoints. In the destination sites (KANS and INDI), the DTNs (D1–8) are also paired in distinct hosts and communicate directly with the local SmartNIC’s router VM (R3–4), without edge-router VMs because no traffic shaping is ever required there. All VMs run Ubuntu 22.04.

The elevation of packets to the EF priority and the enforcement of bandwidth isolation are confined within the data path between the VC endpoints. In fact, FABRIC does not support traffic prioritization between the DTNs and the respective VC terminations (i.e., between S1–8 and R1–2, and between D1–8 and R3–4), so in those portions of the network path the packets of the data transfers may face unpredictable cross-traffic interference (we add the ER VMs to assess the effectiveness of traffic shaping at mitigating the interference impact). Lack of access to performance monitoring counters in the switches of those network segments also prevents the pinpointing of the packet losses that are not captured by counters of the DTN and router VMs. We call those losses non-congestive because they are caused by short-term burstiness and not by extended oversubscription of reserved bandwidth.

For high-capacity tuning of the DTN VMs, we follow best practices for 100 Gb/s TCP [19]. We raise the socket buffer limits from the Linux default of 16 MB to 2 GB, enable jumbo frames, and enable NIC offloading features (TSO, GSO, and GRO) to reduce per-packet processing overhead, while keeping LRO disabled. We further apply system-wide Linux `sysctl` tuning to raise TCP and socket buffer limits, enlarge ingress backlogs, enable MTU probing, disable cached TCP metrics, and set the default queue discipline to Linux `tc-fq`.

On every VM, we disable Linux’s automatic IRQ balancer and manually pin each NIC’s IRQs to a NUMA node to improve packet processing stability. For edge routers (ER1–4) and routers (R1–4), where we explore Linux-kernel and DPDK packet forwarding options, we isolate a set of CPUs for the DPDK applications using `nohz_full`, `rcu_nocbs`, and `isolcpus`, while confining OS housekeeping tasks to separate cores via `housekeeping`. We also pre-allocate 100 instances of 1 GB `hugepages` to support high-performance packet processing.

We pin vCPUs and NUMA-bound memory to the NIC-local socket to minimize cross-socket access and ensure stable high-rate performance. Due to resource constraints when reserving a large number of nodes, CPU pinning and memory binding cannot be applied on a subset of nodes. Finally, we enlarge the NIC ring buffers to 8192 descriptors to avoid packet drops and configure the `tc-fq` queue discipline on sender and receiver interfaces to enable pacing, as recommended in [20].

B. Congestion Control Algorithms

We only evaluate CC algorithms that are designed for high throughput, excluding others that focus on a different metric (e.g., L4S [20] for low packet latency): (a) **TCP CUBIC**, the dominant CC algorithm in today’s Internet [21]; (b) **TCP BBRv1**, widely deployed in practice (22% of top websites and

40% of Internet traffic by volume) [21]; and (c) **TCP BBRv3**, which replaced BBRv2 and is now used for Google’s internal WAN traffic and the google.com and YouTube services [8].

We generate TCP traffic with a multi-threaded version of `iperf3` (v3.19.1), enabling the `--zerocopy` and CPU pinning (`-A`) options to reduce CPU overhead and scheduling jitter. In the experiments with 20 Gb/s VCs, all eight VCs are concurrently active, each transferring a 1 TB file for an FCT value of about 8 minutes. We run experiments with 1 and 10 parallel TCP flows, five times for each configuration. Our reference metric is the *FCT efficiency*, defined as the ratio between the ideal and the measured FCT. We plot the mean over the five runs, adding whiskers for the minimum and maximum samples. The ideal FCT is the file size divided by the bottleneck capacity, adjusted for protocol headers.

C. Data-Path Configurations

As an alternative to the Linux kernel, in some experiments we instantiate the packet forwarding function of the routing VMs as a user-space DPDK application. We actually test two distinct DPDK applications, one providing plain fast forwarding, the other also capable of *shaping* per-VC queues at their reserved HP-WAN rates [22], [23].

In the fast-forwarding application, a polling thread receives packets on the ingress port of the NIC, applies MAC/VLAN headers, and forwards packets in bursts to the egress port buffer. Conversely, the shaper application classifies incoming packets into per-sender queues and releases them to the egress port buffer according to a preconfigured schedule that enforces the desired shaping rates. In both cases a dedicated TX thread transmits the packets out of the port buffer. Every routing VM runs two instances of either application in parallel for the two traffic directions. With Linux kernel forwarding we configure a multi-queue (`mq`) root `qdisc` with per-priority `pfifo` queues. In all routing VM configurations we use large buffers (8BDP) and enable explicit congestion notification (ECN) with 1BDP threshold to avoid local packet losses.

In the topology of Fig. 2, we consider three data-path configurations: (a) Linux kernel forwarding on all routers without shaping; (b) DPDK fast forwarding on all routers; (c) DPDK shaping on the edge routers (ER1-4) with DPDK fast forwarding on the other routers (R1-4). Ideally, with (a) and (b) the L2PTP policer should be the single source of packet loss events and no losses at all should occur with (c). Instead, unexpected packet losses occur in the experiments due to gaps in the user control of the data path. A VC may lose packets to cross-traffic interference in the shallow buffers of the switches between the DTNs and the VC entry points at both ends of the TCP connection and also in the shallow buffers of the HP-WAN path due to collisions with other VCs, even if all VCs are aggressively policed. Virtualization overheads and jitter may also cause uncounted losses in all VMs.

IV. EXPERIMENTAL RESULTS

We design our experiments to answer the following question: which combination of data-path configuration and CC

algorithm provides the most efficient and predictable massive data transfers over public HP-WAN VCs? We first baseline the system performance limits on a reduced topology, then explore the full range of surviving options on the full topology.

A. System Performance Limits

We provision a single 80 Gb/s VC with one sender and one receiver, in line with the logical topology of Fig. 1, and test different configurations of the traffic manager device (instantiated in the R1 router of Fig. 2) to assess their fitness for support of high data rates. For end-to-end transport we use 10 parallel BBRv1 flows. BBRv1 is best suited for identifying system-level bottlenecks because it is relatively insensitive to packet losses and is known to sustain very high sending rates. We evaluate four router configurations: Linux kernel forwarding, with and without traffic shaping (single-queue `tc-htb`), DPDK fast forwarding, and single-queue DPDK shaping. The single-queue shaping rate is 80 Gb/s. Figure 3 plots the average goodput of five 120-second data transfers for each configuration. The Linux `tc-htb` shaper fails to sustain the target 80 Gb/s goodput due to heavy processing overhead, so we exclude it from all the experiments that follow.

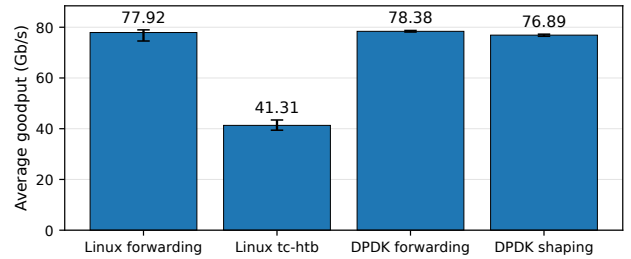


Fig. 3: Goodput performance of router VM configuration options.

Next we run experiments on the 80 Gb/s VC using 10 TCP CUBIC flows and the single-queue DPDK shaper configured with 80 Gb/s shaping rate. While BBRv1 could sustain the target rate (Fig. 3), TCP CUBIC fails to do the same because it misinterprets the non-congestive packet losses as congestion signals (Fig. 4). We remove the CUBIC plots from the next set of results because they reflect the same inferior performance.

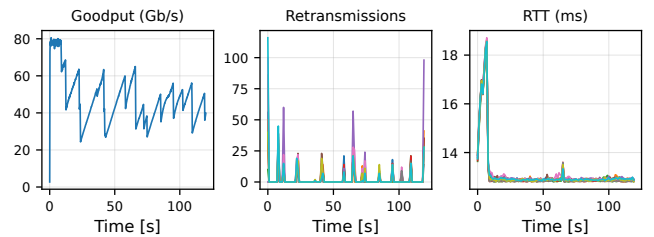
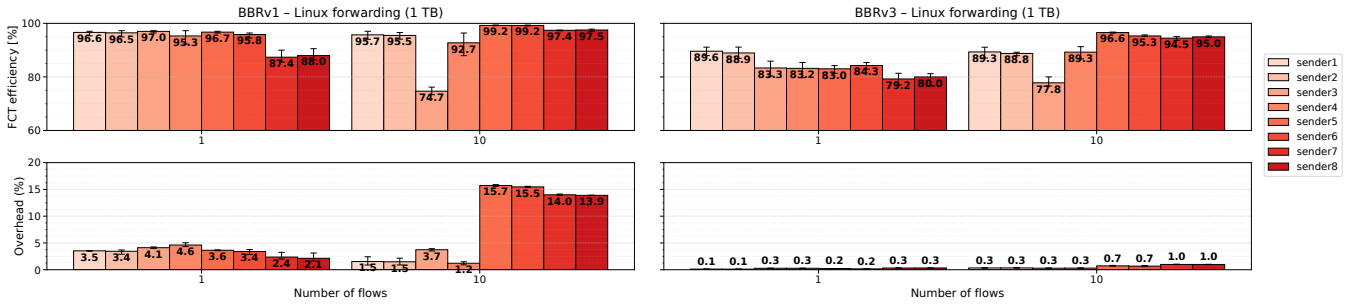


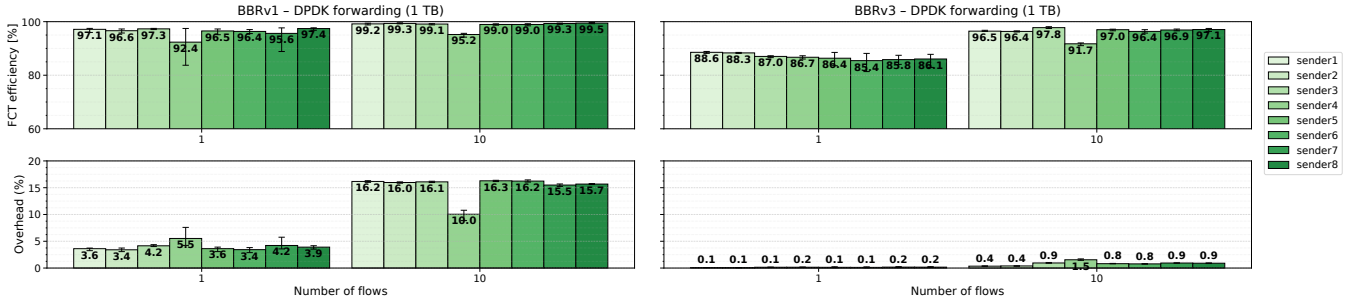
Fig. 4: 10 TCP CUBIC flows with DPDK shaping at 80 Gb/s.

B. Full-Topology Experiments

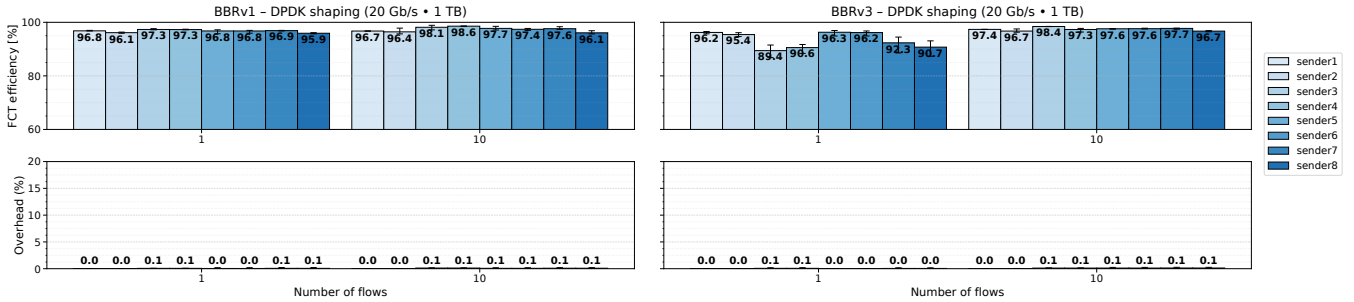
Figure 5 shows the results of our experiments on the full topology of Fig. 2. Each bar in the plots refers to one HP-WAN VC. For each combination of data-path configuration and CC algorithm we run experiments with 1 and 10 flows per VC. The overhead plots on the bottom row of each pair report the extra



(a) BBRv1 and BBRv3 performance with Linux forwarding.



(b) BBRv1 and BBRv3 performance with DPDK forwarding.



(c) BBRv1 and BBRv3 performance with DPDK shaping.

Fig. 5: BBRv1 and BBRv3 performance with different configurations on the routers before the L2PTP tunnel.

bandwidth that the BBR flows consume between the source VM and the VC entry point due to packet retransmissions, expressed as a percentage of the nominal 20 Gb/s of the VC. In the DPDK shaping configuration, the per-VC shapers are set to 20 Gb/s. Our main findings are discussed next.

DPDK shaping is the best data-path configuration. Per-VC shaping at the edge-router VMs (ER1-4) minimizes the burstiness of VC traffic between the TCP senders and the policers, and therefore the chances of packet losses induced by cross-traffic interference. The routers R1-4 operate the plain fast forwarding application to avoid additional restrictions on the throughput of the VCs. DPDK shaping achieves the highest FCT efficiency and predictability, especially with BBRv1, and the lowest bandwidth overhead (0.1%), as a clear indication that it enables the most accurate estimation of the VC bandwidth by the BBR senders. The key benefit of the per-VC shaper is the burstiness minimization for the traffic aggregates that traverse the VCs after crossing the policers.

Linux forwarding relies solely on the hard policers of the HP-WAN VCs to enforce their bandwidth guarantees. It consistently delivers the worst performance (Fig. 5a) in terms of both FCT efficiency (mean value) and predictability (variance). We attribute the performance degradation to the burstiness of high-rate packet forwarding with full traversal of the Linux network stack in a virtualized environment (bare-metal Linux installations are not feasible in FABRIC). The burstiness induces massive packet losses in the uncontrollable data paths between the TCP and VC endpoints (policers included), and most critically prevents the BBR senders from accurately estimating the guaranteed bandwidth of the VCs.

DPDK fast forwarding reduces the forwarding jitter compared to Linux forwarding. The packet loss patterns stabilize, allowing the BBR sources to better estimate their available bandwidth (Fig. 5b). However, the bandwidth overhead becomes even larger than that of Linux forwarding (16.3% maximum vs. 15.7%) because the loss pattern stabilization is

only experienced by the overall traffic aggregates and not by the per-VC aggregates, increasing the frequency of the packet drop decisions by the policers.

BBRv1 yields better predictability than BBRv3. In our setting with entrenched non-congestive packet losses, BBRv1's lower sensitivity to those losses yields more stable FCT efficiency across trials and senders than BBRv3, which instead backs off when the loss rate increases. The loss rate reduction enabled by per-VC shaping allows BBRv3 to match and even outperform BBRv1 for some senders in the 10-flow case. This improvement reflects the BBRv3 redesign of the *ProbeRTT* mode: during a *ProbeRTT* episode, BBRv1 drops the congestion window to only four packets for roughly 200 ms plus one RTT; in contrast, BBRv3 drops it to 0.5 BDP, allowing the sender to transmit at a much higher rate, which improves the overall FCT efficiency when losses are limited. Finally, in non-shaping configurations BBRv3 exhibits much lower bandwidth overhead than BBRv1 at the price of lower FCT efficiency. Together, these results highlight a key trade-off: BBRv1 is more predictable when heavy non-congestive packet losses occur, while BBRv3 can close the gap under data-path configurations that suppress the non-congestive losses.

Over-provisioning the VC rate is not worthwhile. With DPDK shaping we tried to lower the shaping rates of the VCs compared to their HP-WAN reservations (e.g., 15 Gb/s vs. 20 Gb/s). We summarize the results without showing them for space reasons: we measured lower but still relevant packet loss rates and saw no meaningful FCT improvement. BBRv1 still outperformed BBRv3, confirming that FCT predictability mostly derives from robustness to non-congestive losses.

Non-congestive packet losses could not be eliminated in our FABRIC setup. We tried many options for elimination of the non-congestive losses, including per-VC shapers on R1-4 and co-location of those shapers with the senders, yet the losses persisted. Although we could not exactly pinpoint the loss location, experiments with co-located senders and shapers suggest that most losses occur near the TCP receivers. A CC algorithm with minimal sensitivity to non-congestive losses is the best option for achieving predictable massive transfers in public HP-WANs. However, since BBRv1 coexists poorly with loss-sensitive TCP variants, its use must be limited to isolated VCs that do not carry other types of TCP traffic.

Within the bandwidth range of our tests, single-flow transfers are preferable. The results with BBRv1 and DPDK shaping show that single-flow and multi-flow data transfers are practically equivalent. In our experiments, *iperf3* emulates an ideal application for packet distribution and reordering over parallel TCP flows. A practical application may instead introduce overheads that degrade the FCT, making single-flow transfers preferable with VC bandwidth up to at least 20 Gb/s.

V. CONCLUSIONS

We studied the completion-time efficiency and predictability of prominent TCP CC algorithms for massive data transfers over public HP-WANs. Using L2PTP VCs on the FABRIC testbed, we compared three network configurations at the VC

ingress (Linux kernel forwarding, DPDK fast forwarding, and DPDK shaping) and found that per-VC shaping substantially improves FCT predictability and minimizes the bandwidth overhead from packet retransmissions. Combined with per-VC shaping, BBRv1 provides more efficient and predictable file transfers than BBRv3 and CUBIC. Given the challenges posed by the FABRIC data path, especially the frequent occurrence of non-congestive packet losses, the pairing of per-VC shaping with BBRv1 stands out as the most promising option for any other public HP-WAN that supports bandwidth reservations, at least within the 80 Gb/s range of our experiments.

REFERENCES

- [1] Q. Xiong, D. Huang, K. Yao, and C. Lin, "Framework for High Performance Wide Area Network (HP-WAN)," IETF, Internet-Draft draft-xhy-hpwan-framework-02, Jun. 2025.
- [2] InfiniBand Trade Association, "RDMA over Converged Ethernet (RoCEv2) Specification," *InfiniBand Trade Association Specification*, 2014, accessed: 2023-10-05. [Online]. Available: <https://www.infinibandta.org>
- [3] E. Kissel *et al.*, "Efficient Wide Area Data Transfer Protocols for 100 Gbps Networks and Beyond," in *Proceedings of ACM NDM '13*.
- [4] C. Guo *et al.*, "RDMA over Commodity Ethernet at Scale," in *Proceedings of ACM SIGCOMM 2016*, p. 202–215.
- [5] I. Mahmud *et al.*, "Elephants Sharing the Highway: Studying TCP Fairness in Large Transfers over High Throughput Links," in *Proceedings of the SC '23 Workshops (ACM SC-W '23)*, November 2023.
- [6] S. Ha *et al.*, "CUBIC: a new TCP-friendly high-speed TCP variant," *SIGOPS Oper. Syst. Rev.*, vol. 42, no. 5, p. 64–74, July 2008.
- [7] N. Cardwell *et al.*, "BBR: Congestion-Based Congestion Control," *ACM Queue*, vol. 14, September-October, pp. 20 – 53, 2016.
- [8] —, "BBRv3: CCWG Internet-Draft Update," IETF, Tech. Rep., July 2024, IETF 120.
- [9] I. Baldin *et al.*, "FABRIC: A National-Scale Programmable Experimental Network Infrastructure," *IEEE Internet Computing*, vol. 23, no. 6, pp. 38–47, 2019.
- [10] K. Thareja, "Guaranteed QoS and Path-Controlled L2 Network Creation Using EROs in FABRIC," <https://artifacts.fabric-testbed.net/artifacts/7e439627-96be-45e0-ab67-50bb607f06e4>, accessed: 2025-10-13.
- [11] "Data Plane Development Kit (DPDK)." [Online]. Available: <https://www.dpdk.org/>
- [12] M. Gartner *et al.*, "Hercules: High-Speed Bulk-Transfer over SCION," in *2023 IFIP Networking Conference (IFIP Networking)*, 2023, pp. 1–9.
- [13] E. Mutter and S. Shannigrahi, "Science DMZ Networks: How Different Are They Really?" in *2024 IEEE 49th Conference on Local Computer Networks (LCN)*, 2024, pp. 1–9.
- [14] D. King *et al.*, "Current State of the Art for High Performance Wide Area Networks," IETF, Internet-Draft draft-kcrh-hpwan-state-of-art-02, Jul. 2025.
- [15] B. Allcock *et al.*, "Data Management and Transfer in High-Performance Computational Grid Environments," *Parallel Computing*, vol. 28, no. 5, pp. 749–771, 2002.
- [16] B. Tierney *et al.*, "Exploring the BBRv2 Congestion Control Algorithm for use on Data Transfer Nodes," in *Proc. of IEEE INDIS 2021*.
- [17] J. Heinanen and R. Guerin, "A Single Rate Three Color Marker," RFC 2697, Sep. 1999.
- [18] D. L. Black *et al.*, "An Architecture for Differentiated Services," RFC 2475, Dec. 1998.
- [19] M. Hock *et al.*, "TCP at 100 Gbit/s – Tuning, Limitations, Congestion Control," in *2019 IEEE 44th Conference on Local Computer Networks (LCN)*, 2019, pp. 1–9.
- [20] L4S development hub, "Linux kernel tree with L4S patches," <https://github.com/L4STeam/linux>, 2024.
- [21] A. Mishra *et al.*, "The Great Internet TCP Congestion Control Census," *Proc. ACM Meas. Anal. Comput. Syst.*, vol. 3, no. 3, December 2019.
- [22] A. Francini *et al.*, "Lightweight Determinism in Large-Scale Networks," *IEEE Communications Magazine*, vol. 62, no. 12, pp. 120–126, 2024.
- [23] F. B. Sarpkaya and A. Francini, "DPDK-RoutingAwareShaper," <https://github.com/Nokia-Bell-Labs/DPDK-RoutingAwareShaper>, 2025.